Pergamon

Journal of Structural Geology, Vol. 17, No. 2, pp. 279 to 291, 1995

0191-8141/95 $9.50+0.00

0191-8141(94)E0048-4

Folds with axes parallel to the extension direction: an experimental study

DJORDJE GRUJIC and NEIL S. MANCKTELOW

Geologisches Institut, ETH-Zentrum, CH-8092 Zürich, Switzerland

(*Received* 13 *July* 1993; *accepted in revised form* 31 *March* 1994)

Abstract—Experimental studies of single- and multilayer folding have generally considered shortening of layers oriented perpendicular to the maximum extension direction X (i.e. layers parallel to YZ), or in a more limited number of cases, oblique layers still containing the intermediate Y axis. Few experimental studies have considered the case where the extension direction X lies within the layer itself, although in nature folds with axes parallel to X are quite commonly seen. These folds have often been ascribed to passive rotation of fold axes during continued shear, but it has been shown both theoretically and experimentally that active buckle folds can also develop with axes parallel to X.

Single- and multilayer analogue model experiments were performed on planar layers oriented initially perpendicular to the intermediate Y axis, and with the extension direction X lying within the layer itself. All experiments were conducted in plane strain—either in pure shear or simple shear. Paraffin waxes of different melting ranges were used as analogues for rocks with a power-law rheology (stress exponent around 2–3). With a viscosity ratio of *ca.* 30:1, no measurable fold amplification was discernible for shortening of 36% or shear strain of 3.6. Neither domed initial perturbations with circular sections parallel to the layer nor cylindrical perturbations elongate parallel to the initial stretching direction were significantly amplified. Only at much higher viscosity ratios (*ca.* 600:1) did active buckle folding develop. This folding at high viscosity ratio was associated with flow of the matrix in the X direction around the layer, developing a strong linear fabric parallel to X in the matrix immediately adjacent to the layer. The development of this flow discontinuity between matrix and layer may be characteristic of active buckling of layers parallel to XZ, with fold axes parallel to X.

INTRODUCTION

Folds with hinges parallel to the local stretching lineation are a common feature of orogenic belts (e.g. Cloos 1946, Flinn 1962, Milnes 1968, Bryant & Read 1969, Borradaile 1972, Sanderson 1973, Escher & Watterson 1974, Mattauer 1975, Bell 1978, Malavieille 1987, Froitzheim 1992) and a characteristic feature of most low-angle extensional detachment systems (e.g. Spencer 1982, Davis & Lister 1988, Mancktelow 1990, 1992, Mancktelow & Pavlis in press). The stretching lineation may represent the long axis of the total finite strain ellipsoid, developed by superposition of either sedimentary compaction plus tectonic strain (Ramsay & Wood 1973, Mazzoli & Carnemolla 1993) or of multiple tectonic strains (e.g. Huber-Aleffi 1982). In this case, there is no direct kinematic relationship between the fold axes and the lineation. In other cases, however, the incremental stretching direction appears to have been parallel to the fold axes during fold amplification (e.g. Simpson 1982, Klaper 1988, Stünitz 1991, Mancktelow 1992, Gilotti & Hull 1993, Mancktelow & Pavlis in press). It is the development of these structures which is investigated here.

Single- and multilayer fold studies have generally considered shortening of layers oriented perpendicular to the maximum extension direction X (i.e. layers parallel to YZ, e.g. Biot 1959, 1961, Biot *et al.* 1961, Ramberg 1961, 1964, Cobbold 1975, Fletcher 1974, Smith 1975, Abbassi & Mancktelow 1990, 1992, and many others), or in a more limited number of cases, oblique layers still containing the intermediate Y axis (e.g. Treagus 1973, Mainz & Wickham 1978). This is taken to be the usual orientation for fold initiation. As a result, it has been proposed that fold axes now oriented approximately parallel to the stretching direction, X, developed by progressive rotation of the axes away from an initial orientation close to the intermediate axis Y (Sanderson 1973, Escher & Watterson 1974, Williams 1978, Cobbold & Quinquis 1980, Skjernaa 1980). These models all require high strains (e.g. simple shear strain $\gamma > \sim 10$) to achieve near parallelism between fold axes and the bulk stretching direction (X), and assume homogeneous deformation of passive folds (Donath & Parker 1964), in which the folded layering is a passive marker rheologically indistinguishable from the surrounding matrix. In these passive models, small initial irregularities are kinematically amplified during progressive strain (Cobbold & Quinquis 1980) and may develop characteristic sheath-fold geometries. However, many natural folds developed with axes parallel to X bear no resemblance to sheath-folds—they can be quite open upright structures without evidence for very high strain during their development (e.g. Spencer 1982, Mancktelow & Pavlis in press).

For active (or dynamic) folding, the layering has distinct rheological properties and is more resistant to deformation than the matrix. This leads to a heterogeneous distribution of deformation and the development of a buckling instability. The development of sheath folds in mechanically active layers will be hindered by the necessity for significant in-plane strains within the stronger layer. If, as is to be expected in most cases, the folds behave actively (Carreras *et al.* 1977,

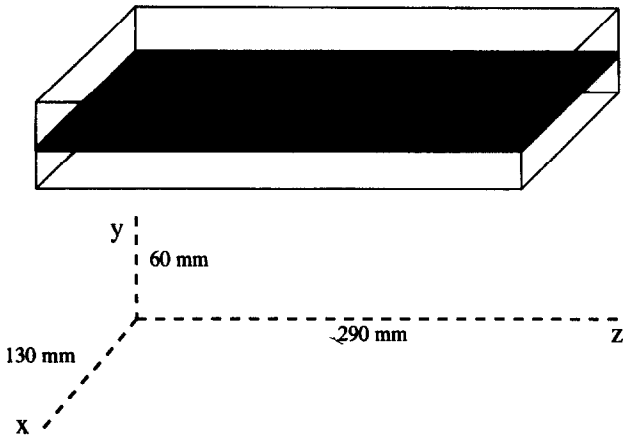

Fig. 1. Schematic diagram of the model and deformation geometry for pure shear experiments, showing the orientation of the initially flat, planar layer with respect to the *XYZ* bulk strain axes of the imposed deformation.

Hudleston 1977) then some degree of hinge migration (Treagus & Treagus 1981) should occur during the rotation of fold axes.

Ramberg (1959, fig. 3), Flinn (1962) and Ramsay (1967, fig. 3–54) proposed that folds develop perpendicular to the shortening direction within the layer and therefore, for the Field 2 geometry of Ramsay (1967, fig. 3–54), will also develop parallel to the extension direction of the 2D strain ellipse within the layer. Since then, only a few authors have considered models where active buckle folds initiate parallel to the extension direction: in pure shear (Watkinson 1975), simple shear (Wilcox *et al.* 1973, Odonne & Vialon 1983), or more general 3D strain histories (Treagus & Treagus 1981, Ridley 1986, Ridley & Casey 1989). Recently, two theoretical studies have considered the initiation of buckle folds with axes parallel to *X* (Fletcher 1991, James & Watkinson 1994), providing a good basis for further experimental investigation of the growth of these structures to finite amplitude. This paper reports the results of such an experimental study using analogue materials to investigate active buckling of single- and multilayers oriented parallel to the *XZ* principal plane for pure and simple shear boundary conditions.

EXPERIMENTAL PROCEDURE

Introduction

All experiments were performed under plane strain conditions with single- or multilayers oriented parallel to the *XZ* plane of the imposed deformation (Fig. 1). For most experiments, the opaque matrix to either side of the layer(s) hindered direct observation of the developing folds and the fold geometry could only be observed at the end of an experiment once the matrix material had been carefully removed. However, a few experiments were also performed with a transparent polymer as the upper matrix, so that fold development could be continuously monitored.

Deformation conditions

Two model deformation rigs were employed, to study folding under conditions of pure and simple shear. In the pure shear rig (Mancktelow 1988a), all models were shortened by 36% at a constant natural strain rate of $\dot{\varepsilon} = 5.0 \times 10^{-6}\ s^{-1}$ and a confining stress σ_3 of 0.03 MPa. Differential stress (σ_1–σ_3), confining stress, temperature and strain rate were all recorded during the experiments. In the simple shear rig (Ildefonse & Mancktelow 1993), all models were sheared to $\gamma = 3.8$ at a constant shear strain rate of $\dot{\gamma} = 1.5 \times 10^{-5}\ s^{-1}$. The experiments were conducted under two constant temperature conditions, namely: (a) lower viscosity ratio experiments (≈30:1) at 24 ± 0.1°C, (b) higher viscosity ratio experiments (≈600:1) at 30 ± 0.1°C. As a control on the reproducibility of results, experiments were performed at least twice.

Modelling materials

Two different paraffin waxes were used in the current experiments. The softer wax forming the matrix has a melting range of 46–48°C (Merck, 7151), whereas the wax representing the competent layer has a melting range of 50–52°C (Fluka, 76229). Because the mechanical properties of paraffin wax are very temperature sensitive, two sets of calibration experiments were performed corresponding to the temperature conditions of model experiments, that is 24 ± 0.1°C and 30 ± 0.1°C. The two waxes were calibrated at these temperatures using a rheometer (BOHLIN CS-50) and the pure shear deformation rig itself (Mancktelow 1988b). For the strain-rates of the experiments, the wax used for the matrix has a power-law rheology with a stress exponent of $n \approx 2.7$ over the temperature range 24–25°C. Under the same conditions the layer has a stress exponent $n \approx 2.4$ (Mancktelow 1988b). In this temperature range (24–25°C), the waxes used for the layer and the matrix have an effective viscosity ratio of *ca.* 30:1. Above 26–28°C, the matrix material exhibits a marked weakening, which approximates to the α–β phase transition for this paraffin wax (Mancktelow 1988b). The corresponding transition for the layer paraffin wax occurs at around 34°C. Consequently, at 30°C this results in a very high viscosity ratio between layer and matrix of about 600:1. Similar high viscosity ratios have been used in some other analogue experiments on fold development (e.g. Odonne & Vialon 1987), and such high viscosity ratios may also be geologically reasonable where layer and matrix have very different mechanical behaviour (cf. Biot 1961, Kirby 1985, fig. 5).

To allow continuous observation of the layer, a few models were prepared where the upper half of the matrix was a transparent polydimethyl-siloxane (PDMS—SGM 36 by Dow Corning, Weijermars 1986). Under experimental conditions, the PDMS has a linear

viscous rheology with viscosity of *ca.* 4.5×10^4 Pa s (Weijermars 1986, fig. 11). These composite models are used as an aid to understanding the progressive development of folding in the models constructed of wax alone.

Model preparation

The paraffin wax used for the matrix was melted and poured into moulds. After cooling, the paraffin wax was cut into two halves and, if needed, a negative of an initial perturbation was cut out in the middle of one of the halves. Meanwhile, a 4 mm-thick flat plate of the higher melting range paraffin wax was prepared. For the experiments where the layer had an initial perturbation the layer was heated in an incubator until soft and moulded between the pre-formed matrix blocks. The assembled model was then machined into its final shape ($290 \times 120 \times 60$ mm for pure shear and $490 \times 120 \times 50$ mm for simple shear) and loaded into the deformation rig. The initial bonding between layer and matrix was very weak, corresponding to the assumption of *easy slip* between layer and matrix in some folding theories (e.g. Biot 1959, 1961). However, it has been shown (Biot 1959, Smith 1975, Mancktelow & Abbassi 1992, fig. 5) that at high viscosity ratio (*ca.* >100:1) there should be no significant difference in growth rate for the two extremes of perfect slip and perfect adherence between layer and matrix. After experimental deformation, one half of the matrix was removed to allow 3D observation of the folded layer surface (Figs. 2 and 3). To study the fabric development, samples of paraffin wax were also observed under the scanning electron microscope (Fig. 4). In the few models where PDMS was used, the lower half of the matrix and the layer were first loaded into the deformation rig, then the rest of the space filled with PDMS. After waiting for the inevitable air bubbles in the PDMS to surface, the experiments were conducted under the same conditions as the models made entirely of wax.

EXPERIMENTAL RESULTS

Pure shear – single layer

Two sets of experiments were carried out with a single layer subject to pure shear deformation (Fig. 1). In the first set of models the layer was 'perfectly' planar with initial perturbations <0.05 mm, i.e. <0.0125 of the layer thickness (Fig. 2). With a moderate viscosity ratio of *ca.* 30:1, the layer deformed homogeneously in a manner similar to the matrix and no buckle folds developed (Fig. 2a). Folds only formed for models with a high viscosity ratio (*ca.* 600:1). The resulting folds have their axes parallel to the stretching direction, have low amplitudes even at 36% bulk shortening and are sub-cylindrical (Fig. 2e). Folds initiate in the middle of the model and propagate toward its edges. The layer parallel strain, in both Z and X directions is 54% of the bulk strain, which implies that the matrix must have flowed around the layer, as is clear from Fig. 2(e). The spacing of folds is expressed by the arclength/thickness ratio, defined as the total arc length measured along the layer divided by the number of folds and normalized against the layer thickness (Sherwin & Chapple 1968, Fletcher & Sherwin 1978, Hudleston 1986, Abbassi & Mancktelow 1990). The arclength/thickness ratio is around 13.7 (Fig. 5a), which is much less than the ratio in the case of folding under identical boundary conditions but with the layer initially oriented parallel to the YZ plane of the imposed bulk strain (Fig. 5b). For such models, the folds have a large arclength to thickness ratio of around 26.9 and there is very little layer-parallel shortening (<1%), as predicted theoretically (Ramberg 1964).

Experiments with a transparent upper half for the matrix (PDMS) allow a direct comparison between the progressive buckling of a layer parallel to XZ and that of a layer with the 'usual' orientation (i.e. parallel to YZ). There are two sequential mechanisms, layer-parallel strain and buckling. Initially the deformation is accommodated more-or-less homogeneously, but with the onset of buckling the rate of further layer-parallel strain in the layer diminishes rapidly. For continued buckling of a layer initially oriented parallel to XZ, there is effectively no further stretching of the layer parallel to the fold axis. This stretch must be accommodated by flow of the matrix around the layer in the X direction (i.e. parallel to the fold axes), to maintain constant volume.

A second set of model experiments were performed with viscosity ratio *ca.* 30:1 under identical conditions to the first, except that an initial perturbation of finite amplitude was introduced into the layer. Several initial geometries were investigated. In the first case, the isolated perturbation had initial limb dips of 12°, an amplitude of 0.75 of the layer thickness and a spherical-cup shape. The introduced initial perturbation did not amplify to form folds, but was passively deformed in accordance with the homogeneous strain distribution in the layer (Fig. 2b). In the second case, the initial perturbation was cylindrical and elongate parallel to the X axis, with initial limb dips of 15° and an amplitude of 0.5 of the layer thickness. Again no significant amplification was observed during the experiment (Fig. 2c). In the third case, initial 'folds' with limb dips of 45° and an amplitude of 1.5 of the layer thickness (Fig. 6a) were introduced. As a result of the experimental deformation, the initial fold shapes were extended and slightly boudinaged parallel to their axes by the same amount as the bulk strain (Fig. 2d), but in the YZ section perpendicular to their axes they underwent only homogeneous shortening perpendicular to their axes. This produced a tightening of the initial fold profiles and consequent steepening of fold limbs, but no measurable increase in fold amplitude (Fig. 6b).

Pure shear—multilayer

The regularly stacked multilayer consisted of three competent and two incompetent layers embedded in a

matrix of the same viscosity as the incompetent layers (Fig. 7). The layer thickness was 2 mm making the whole stack thickness 10 mm. The thickness ratio of incompetent to competent layers (d_2/d_1) was 1. The experiments were conducted under the same boundary conditions as for the single layer experiments. Depending on whether the viscosity ratio was low or high, these models correspond respectively to Model A and Model C multilayers of Ramsay & Huber (1987, p. 418).

Similar to the single layer models, in the lower viscosity ratio experiments no folds developed and the layers were deformed solely by layer parallel strain consistent with the bulk imposed strain. Folds only developed in the high viscosity ratio experiments. The arclength/thickness ratio for the individual layers was *ca.* 21.5, or 4.3 for the whole multilayer.

Simple shear

Models of similar initial geometry to those deformed in pure shear were also deformed in simple shear (Fig. 8). Non-linear viscous materials do not transfer shear stress homogeneously (Hobbs 1972), and consequently strain is concentrated at the model boundaries. These boundary effects (Fig. 3, cf. Biot 1968, p. 133) make it generally more difficult to perform realistic experiments in simple shear. However, results from experiments with simple shear boundary conditions are important for comparison with natural rotational deformation histories and with the results from pure shear experiments. Folds again developed only at high viscosity ratio (Fig. 3d). Fold amplitudes were generally similar to those of folds developed in pure shear. The introduced perturbations had the same shape as in the models for the pure shear experiments and the results were also comparable (Figs. 3b & c): neither equiaxed initial perturbations nor elongate cylindrical perturbations with axes parallel to the initial X direction (i.e. 45° to the shear plane) showed any discernible amplification, but were simply passively modified in accord with the bulk strain within the layer. The axis of the introduced cylindrical perturbation remained fixed to the same material points throughout the simple shear deformation and rotated as a material line. As a result, it did not track the direction of the finite stretching direction, X, during progressive simple shear. Extension parallel to the fold axis resulted in boudinage of the fold hinge, and disjointed segments of the hinge rotated as rigid blocks to develop an en échelon form (Fig. 3c).

To observe the progressive development of folds a high viscosity ratio model was prepared where the upper half of the matrix was made of PDMS. Similarly to the experiment in pure shear, the layer first undergoes an initial homogeneous strain (to a simple shear strain of $\gamma \approx 0.2$), which effectively ceases with the onset of buckling. Due to the strain localization on the boundaries, the folds initiate near the short edges of the model (Fig. 3d). The folds propagate toward the middle of the model, but in the initial stages when they have low amplitudes it is difficult to determine their orientation accurately. However, axes of the later folds developed away from the boundaries tend to form parallel to the incremental stretching direction of the bulk imposed strain (rather than parallel to the already existing folds) and progressively rotate towards the finite stretching direction. In the course of this process, the fold hinges remain attached to the same material points in the layer (i.e. there is no appreciable hinge migration), which results in shear along the axial planes. This shear is antithetic to the bulk imposed shear and requires discontinuities along the fold axis (e.g. boudinaged folds or normal faults), which is characteristic of a transtensive shear geometry.

DISCUSSION

Comparison between experimental and theoretical results

Active fold amplification was not observed in any of the experiments with layers of lower viscosity contrast (*ca.* 30:1). At first sight, these observations are not in full accord with the theoretical results of Fletcher (1991) and James & Watkinson (1994). Fletcher (1991) notes that dome-and-basin-like initial perturbations should not actively amplify. This is in agreement with the current experiments. He also notes that waveforms with axes parallel to Z in a layer oriented parallel to XZ should actually deamplify. This has been observed in the refolding experiments of Grujic (1993). However, both Fletcher (1991) and James & Watkinson (1994) conclude that sinusoidal waveforms with axes parallel to the X axis should actively amplify. The initial non-dimensional growth rate should be one half the rate for the same waveform in the most favoured orientation for folding, namely with the axis parallel to Y in a layer oriented parallel to YZ. As noted by Fletcher (1991), this halving of the growth rate results in a very dramatic reduction in the finite amplification of initial perturbations, due to the exponential form of the relationship. For example, with a dynamic growth rate of 30 in the YZ layer orientation (consistent with values measured by Abbassi & Mancktelow 1992 for the same materials and conditions), 15% shortening would produce amplification (A/A_o) of a sinusoidal irregularity in an XZ layer that is only one tenth of that of the same irregularity in a YZ layer (Fig. 9, natural strain $\approx$0.15). For a 30:1 viscosity ratio, the amplification of irregularities in a single layer oriented parallel to YZ is already not very dramatic (cf. Abbassi & Mancktelow 1992). For the XZ layer orientation, the amplification of the cylindrical initial perturbations may simply be too small to be observed in the experiments. It is only at the much higher growth rates associated with the high viscosity experiments that fold amplification is clearly observed.

The theoretical studies of Fletcher (1991) and James & Watkinson (1994) conclude that changing the layer orientation should have no affect on the value of the 'dominant wavelength' (i.e. the wavelength with the fastest growth rate), only on the magnitude of the

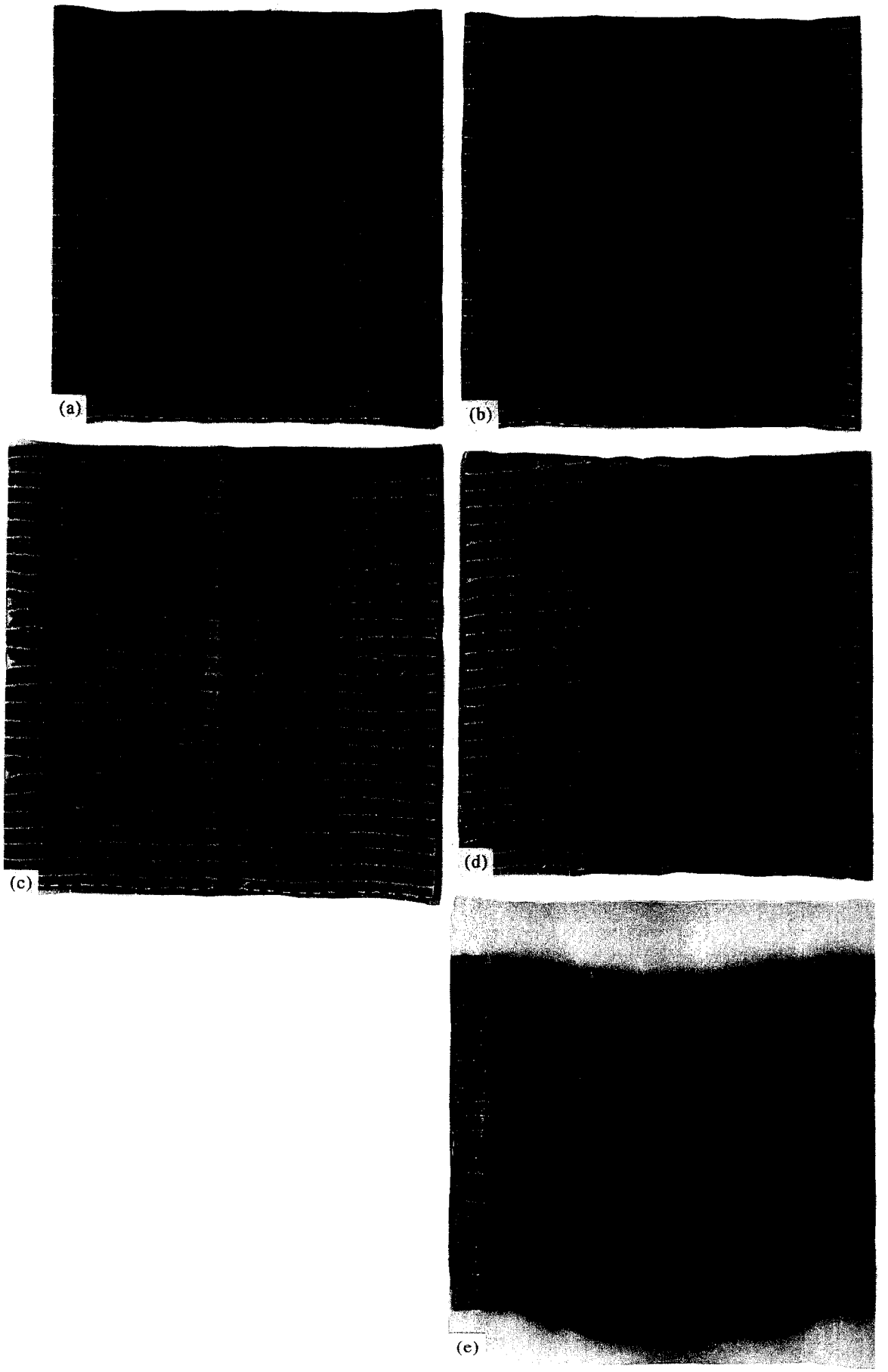

Fig. 2. Photographs of layer surfaces taken at 36% shortening in pure shear, seen in the XZ plane: (a) model with viscosity ratio 30:1 and an initial planar layer, (b) model with viscosity ratio 30:1 and an initial domed perturbation, (c) model with viscosity ratio 30:1 and an initial cylindrical perturbation, (d) model with viscosity ratio 30:1 and initial folds, (e) model with viscosity ratio of *ca.* 600:1 and an initial planar layer. The initial undeformed spacing between the grid lines in all models was 5 mm.

Fig. 3. Photographs of layer surfaces deformed in simple shear taken at $\gamma = 3.8$, seen in the XZ plane: (a) model with viscosity ratio 30:1 and an initial planar layer, (b) model with viscosity ratio 30:1 and an initial domed perturbation, (c) model with viscosity ratio 30:1 and an initial cylindrical perturbation, (d) model with viscosity ratio of *ca.* 600:1 and an initial planar layer. The initial spacing between the grid lines in all models was 5 mm in the undeformed state.

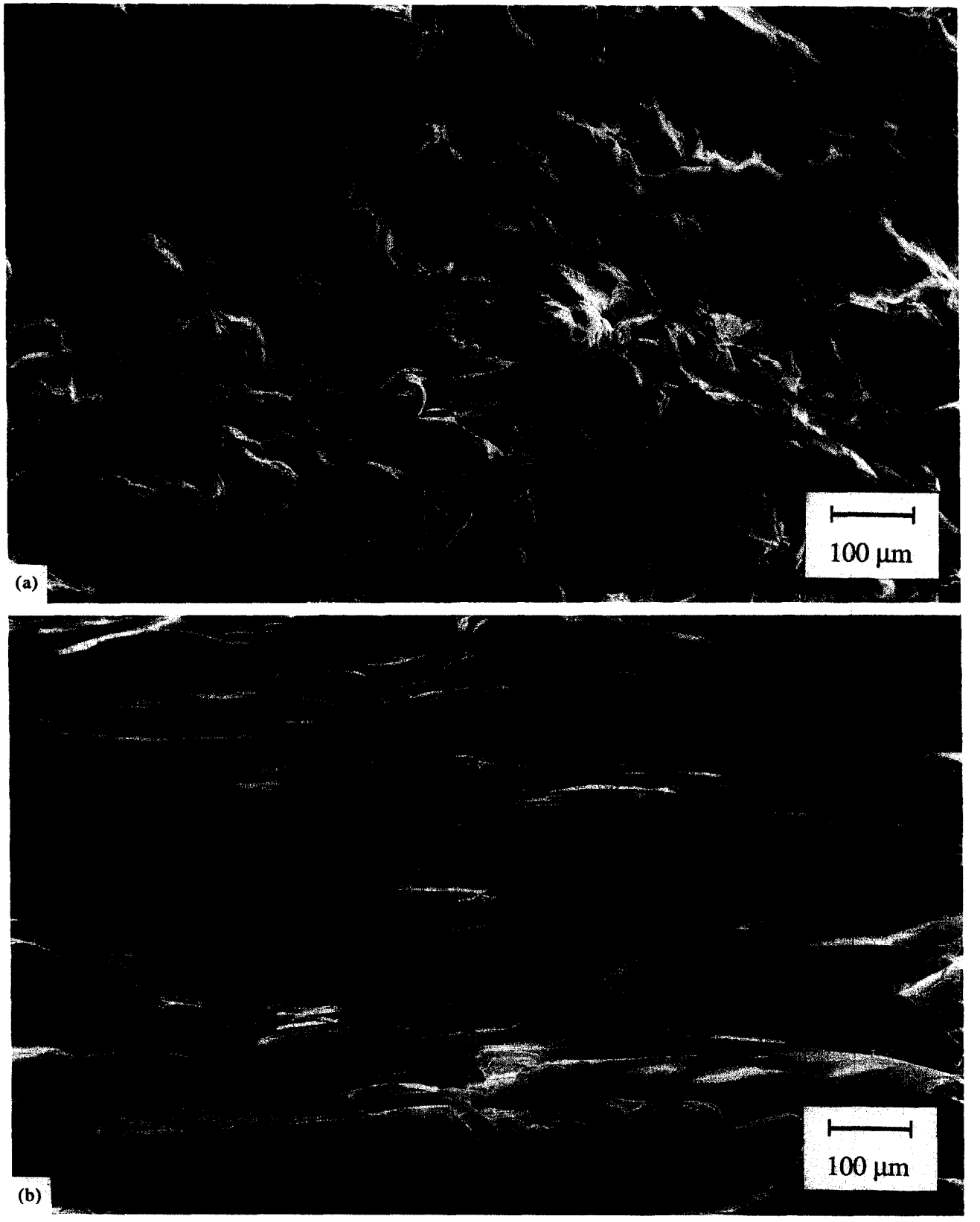

Fig. 4. Development of a strong 'mineral' lineation due to the flow of the matrix around the layer. SEM secondary electron images of paraffin wax in the matrix: (a) before; and (b) after the experimental deformation in pure shear. Approximately XZ plane, about 4 mm from the interface. Scale bar 100 μm.

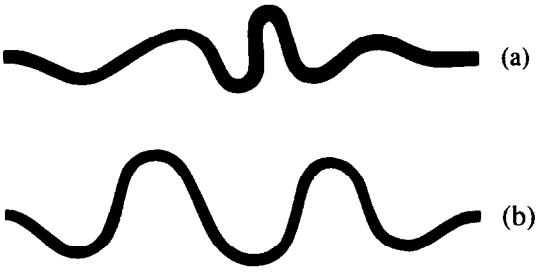

Fig. 5. Cross-sections of folds at 36% shortening in pure shear: (a) folds with axes parallel to the stretching direction, developed in a layer initially parallel to the *XZ* plane of the imposed bulk strain, viewed in the *YZ* plane; (b) folds developed in a layer originally parallel to the *YZ* plane of the bulk imposed strain, viewed in the *XZ* plane. Both experiments were conducted under identical boundary conditions and with same initial layer thickness of 4 mm.

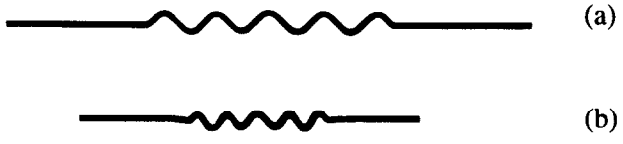

Fig. 6. Cross-sections of folds deformed in pure shear: (a) initial folds with axes parallel to the stretching direction, viewed in the *YZ* plane: (b) same folds at 36% shortening in pure shear, viewed in the *YZ* plane (cf. Fig. 2d). The initial folds were homogeneously shortened perpendicular to their axes but no extension occurred in the *Y* direction. This resulted in fold tightening and apparent but no effective fold amplification.

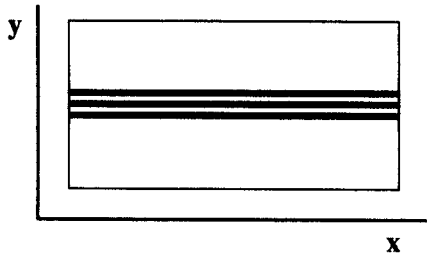

Fig. 7. Schematic diagram of multilayer model geometry.

growth rates themselves. However, in the high viscosity contrast experiments where buckle folds develop spontaneously, the arclength/thickness is considerably lower for layers oriented parallel to *XZ* than for layers oriented parallel to *YZ* (Fig. 5). This discrepancy remains to be clarified.

Interrelation between folding and boudinage of the layer, and flow in the matrix

At initiation and during the initial low limb-dip stages of fold growth, the amplification of buckle folds is exponential (Fig. 9, e.g. Biot 1961, Chapple 1968). Consequently there is always an initial period when the layer undergoes a homogeneous strain together with the matrix before the rate of fold amplification is itself sufficient to accommodate the layer shortening (Hudleston 1973, Abbassi & Mancktelow 1992). If the fold amplification rate is low, due to low rheological contrast between layer and matrix or because of initial layer orientation (such as in the current experiments with the layer parallel to *XZ* and viscosity ratio *ca.* 30:1), then this initial homogeneous strain component in the layer can be quite important. For high amplification rates (e.g. the experiments with high viscosity ratio), folding is more rapidly established and the 'explosive' exponential growth rate is accompanied by an equally dramatic decrease in the rate of layer parallel strain. In the high viscosity contrast experiments, there is effectively no further stretching parallel to the fold axes in the competent layers, once folds have grown to an observable size. Buckle folding results in an overall shortening of the layers's median surface perpendicular to the fold axis and an extension perpendicular to this median surface. Buckling in itself cannot produce an extension parallel to the fold axis. For a layer initially oriented parallel to *XZ*, this does not accord with the imposed bulk plane strain—extension parallel to the fold axes is required. The stretch in the *X* direction can be taken up in the matrix but not in the actively folding layer. However, such an implied displacement gradient (i.e. shear) between layer and matrix in the *X* direction is only possible if the layer is of finite length in this direction (e.g. Smith 1975, fig. 2). In the experiments this is indeed the case, and the matrix flows around the layer once folding initiates, so that overall extension parallel to *X* in the layer is less than in the matrix. In nature, this will only be possible if the layering is broken by boudinage or faulting on some scale (e.g. Ramsay 1967, fig. 3–54, Field 2). The dismemberment of the layer reduces the length to width ratio of the layer in the *X* direction and thus facilitates the flow of matrix past the layer. The *X*-axis parallel folding and the break-up of the layer are linked processes, neither of which can occur without the other.

The heterogeneous flow of the matrix around the layer can result in the development of a strong linear fabric, which is seen in experimental models as a marked alignment of needle-shaped wax crystals (Fig. 4). Amplification of folds in the competent layer in the *Y* direction must be accommodated by a corresponding contraction in the *Y* direction in the adjacent matrix in order to maintain the plane strain boundary conditions. The 3D strain geometry in the zone of contact strain of the matrix will therefore be constrictional. In field examples, the fold axes in more competent layers would thus be seen to be parallel to a particularly well-developed stretching lineation in the immediately adjacent less competent matrix.

A good field example of folding with axes parallel to the stretching direction where folding and boudinage of the competent layer are closely linked is seen in Fig. 10, from the Canavese metasediments of the Insubric line in the Valle Loana (Italy). The synform axis is parallel to the local and regional stretching lineation (Schmid *et al.* 1987). The axes of the three boudins in the competent dolomitic layer are perpendicular to the fold axis and lie in the fold axial plane that parallels the mylonitic foliation (Schäppi 1985). A marked concentration of strain on the competent layer (dolomite) boundary suggests flow of the matrix around the layer.

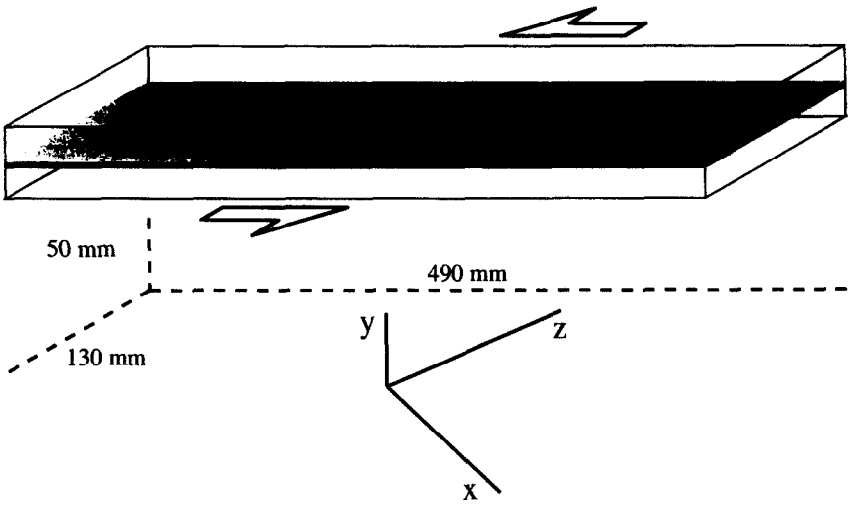

Fig. 8. Schematic diagram of the model and deformation geometry for simple shear experiments, showing the orientation of the initially flat, planar layer with respect to the *XYZ* bulk strain axes of the imposed deformation.

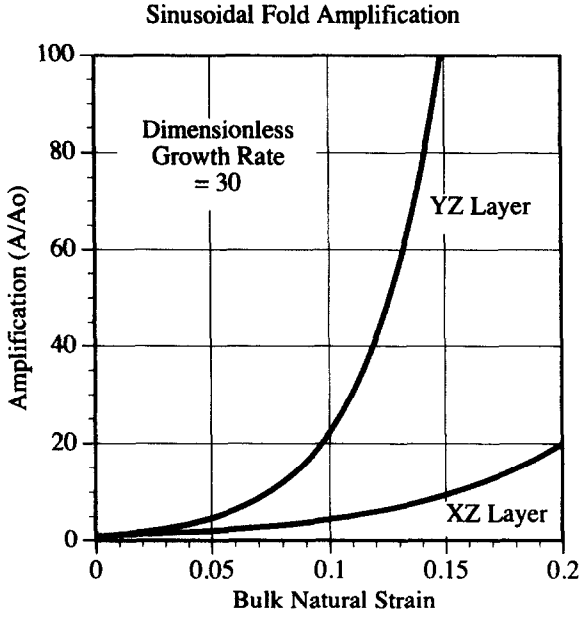

Fig. 9. Comparison of the amplification of folds in layers oriented parallel to *YZ* and to *XZ*. The non-dimensional growth rate is q. For orientation *YZ*, the ratio of current to initial amplitude is given by $(A/A_O) = \exp[(1 + q)\varepsilon]$, where the '1' represents the effect of kinematic amplification, whereas for *XZ*, $(A/A_O) = \exp[(q/2)\varepsilon]$, following Fletcher (1991). The value $q = 30$ corresponds to the measured experimental growth rate of the fastest growing sinusoidal component in experiments with layers parallel to *YZ*, for the same materials and deformation conditions as the current experiments (see Abbassi & Mancktelow 1992, fig. 14).

Superposed folding

In repeated folding there are many geometrical situations which would favour the development of folds parallel to the extension direction. However, in most cases it is only the second phase folds that contain a component of stretching along their axes, due to the greater range of initial orientation of the layering relative to the superposed 3D strain ellipsoid and because layers rotate through different orientations during their deformation history. Many of these orientations may involve a component of stretch in the layer.

The strain distribution on the layer surface in fold interference patterns has been discussed by Ghosh (1970, 1974) and Grujic (1992). Considering only the concentric longitudinal strain it has been shown that both the axial ratio of the strain ellipses and the orientation of their major axes will vary from place to place over the superposed fold surface. For noncoaxial refolding (Type 1 and Type 2 interference patterns, Ramsay 1967, pp. 520–521), there is always a component of stretching parallel to the second phase fold axes because the limbs of initial folds are in the Field 2 of Ramsay (1967, fig. 3–54). The angle between the second fold axes and the bulk strain ellipsoid axes depends on the initial fold interlimb angle. In the Type 1 interference strain geometry (this strain geometry refers to the orientation of the initial fold hinge and axial plane with respect to the *XYZ* bulk strain axes of the second deformation), the initial fold axial planes are parallel to the *XZ* plane of the bulk superposed strain ellipsoid, while the second phase fold axes lie in the *XY* plane. Due to the passive amplification of the initial fold in this strain geometry (Grujic 1993), the second phase fold axes progressively approach the *X* strain axis as the initial fold limbs rotate into the *XZ* plane. In the Type 2 interference strain geometry, the second phase fold axes also lie in the *XY* plane, but the initial fold axial planes are parallel to the *YZ* plane. During progressive deformation, the second phase fold axes passively rotate into the stretching direction inasmuch as the initial folds deamplify (Grujic 1993).

In contrast, for coaxial refolding (Type 3 interference pattern, Ramsay 1967, pp. 520–521) the longest axis of the *finite* strain ellipsoid (of prolate or oblate geometry) may also be parallel to the fold axes, but this total strain geometry has no kinematic significance relative to the strain increments which produced the folding and refolding.

Folding of layers in general orientations oblique to principal axes

In the absence of important initial irregularities (Abbassi & Mancktelow 1990) or linear anisotropy

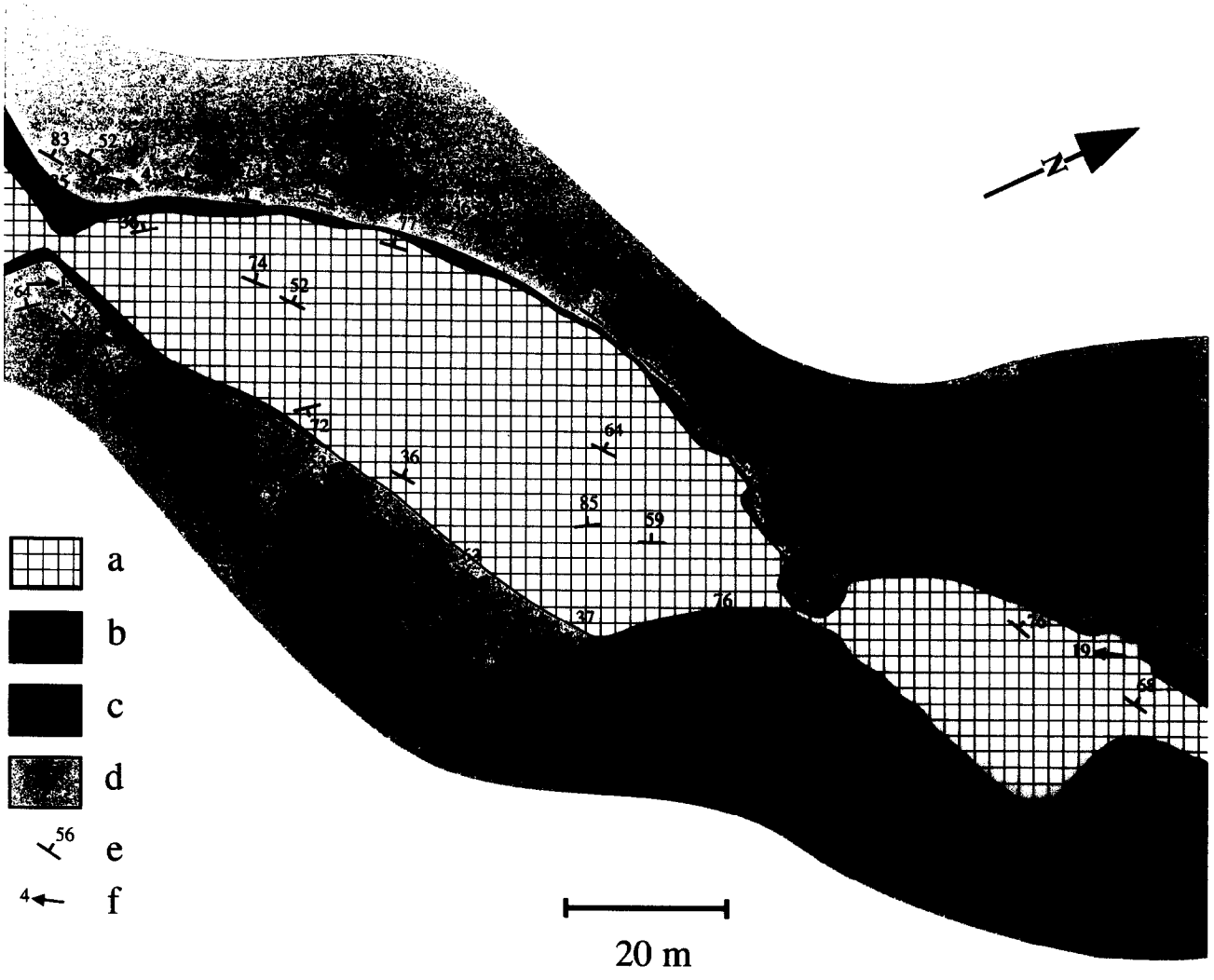

Fig. 10. Outcrop map of a boudinaged synform in Valle Loana, Italian Alps. (a) Marbles, (b) highly deformed rocks, (c) sandstones, (d) schists, (e) schistosity with angle of dip, (f) lineation with angle of plunge. After Schäppi (1985).

(Cobbold & Watkinson 1981, Watkinson & Cobbold 1981), fold geometry and fold orientation are largely determined by the original orientation of the pre-existing rheological layering or planar anisotropy with respect to the shortening or shear direction (e.g. Ramsay 1967, Talbot 1970, Escher & Watterson 1974, Skjernaa 1980, Treagus & Treagus 1981, Ridley & Casey 1986, Ramsay & Huber 1987, Froitzheim 1992). A variable original orientation of the layering or anisotropy results in a correspondingly variable orientation of fold axes—fold axes strictly parallel to Y or X axes of the bulk imposed strain are only end-members. The determining feature both for geometry and orientation is the shape of the 2D strain ellipse parallel to the layer or plane of anisotropy (Ramsay 1967), which is itself a section through the bulk 3D strain ellipsoid modified by refraction at rheological boundaries (e.g. Treagus 1972, 1973, Treagus & Sokoutis 1992). For 2D strain ellipses for which one principal axis is shortened while the other is extended (i.e. Field 2 of Ramsay 1967, fig. 3–54), folds will develop with axes perpendicular to the shortening direction within the layer (Ramberg 1959, Flinn 1962, Ramsay 1967, Treagus & Treagus 1981, Ridley & Casey 1986) and thus parallel to the extension direction. However, fold amplification rates are smaller than for a layer parallel to the YZ plane, as shown by the current experimental study, the analytical results of Fletcher (1991) and James & Watkinson (1994), and the numerical simulation of asymmetric folding by Anthony & Wickham (1978). For this reason, higher viscosity ratios and/or larger initial perturbations are needed for fold initiation when the rheological layering is oblique to the bulk strain axes. Layering parallel to the XZ plane will undergo much larger layer-parallel strain than expected from theories and experiments considering initial layer orientation parallel to YZ (e.g. Biot 1961, Hudleston 1973). This implies that for general layer orientations there is a more important component of initial homogeneous strain before folding predominates and the use of fold shape as an indicator of the rock rheology (e.g. Hudleston & Lan 1993) may not be reliable when the layering was not initially parallel to the XZ plane (which is not always easy to determine from observations in the deformed state).

As noted by Ramsay (1967, fig. 4–25), Field 2 strain geometries in layers are the most general and presumably most common situation. Folds, therefore, should often have a component of stretching parallel to their

axes. This does not imply that the fold axes are strictly parallel to the longest axis of the bulk strain (X). The necessary flow of the matrix around the competent layer parallel to the stretching component in the layer may cause a strong lineation in the immediately adjacent matrix (Figs. 4 and 10), falsely suggesting a large bulk stretch exactly parallel to the fold axes.

CONCLUSIONS

The current series of analogue model experiments have considered the development of active buckle folds with axes parallel to the principal elongation direction X for moderate (~30:1) and high (~600:1) effective viscosity ratios under both pure and simple shear conditions. Whereas folding at high viscosity ratios nucleates without the introduction of an initial finite amplitude perturbation in the layer(s), amplification of folds in the lower viscosity ratio experiments was not observed, even for cylindrical initial perturbations parallel to X. It would seem, therefore, that the development of regular wavetrains of high amplitude folds with this orientation, as have been described from many regions (e.g. Bartley *et al.* 1990, Urai *et al.* 1990, Yin 1991, Mancktelow & Pavlis in press) may imply high effective viscosity contrasts between the folded layers and/or non-plane strain conditions, with a component of extension perpendicular to the fold axis (i.e. an overall oblate or flattening strain).

The analogue models suggest that folding with axes parallel to the stretching direction within the layer may only occur if the layer is discontinuous, either originally or due to concomitant boudinage, thus producing a flow discontinuity in the direction of the fold axes at the matrix/layer interface. It is tentatively proposed, as a spur to further work, that this discontinuous flow geometry may be important on a wide range of scales from individual boudinaged mesoscopic folds (e.g. Ramsay & Huber 1983, fig. 4.12B) to folds in low-angle detachment systems (e.g. Mancktelow & Pavlis in press), where the more competent 'layer' could represent the strong middle crust.

Acknowledgements—We thank M. Casey, M. Genter, T. Pavlis and J. Ramsay for stimulating discussions on folding and faulting. The manuscript benefited from thoughtful reviews by J. Cosgrove, S. Treagus and J. Watkinson. Financial support from the ETH Research Credit 2-77-652-92 and Schweizerischer Nationalfonds Project 0-20-154-86 is gratefully acknowledged.

REFERENCES

Abbassi, M. R. & Mancktelow, N. S. 1990. The effect of initial perturbation shape and symmetry on fold development. *J. Struct. Geol.* **12**, 273–282.

Abbassi, M. R. & Mancktelow, N. S. 1992. Single layer folding in non-linear materials—I. Experimental study of fold development from an isolated initial perturbation. *J. Struct. Geol.* **14**, 85–104.

Anthony, M. & Wickham, J. 1978. Finite element simulation of asymmetric folding. *Tectonophysics* **47**, 1–14.

Bartley, J. M., Fletcher, J. M. & Glazner, A. F. 1990. Tertiary extension and contraction of lower-plate rocks in the central Mojave metamorphic core complex, southern California. *Tectonics* **9**, 521–534.

Bell, T. 1978. Progressive deformation and reorientation of fold axes in a ductile mylonite zone: the Woodroff thrust. *Tectonophysics* **44**, 285–320.

Biot, M. A. 1959. On the instability and folding deformation of a layered viscoelastic medium in compression. *J. Appl Mech.* **E26**, 393–400.

Biot, M. A. 1961. Theory of folding of stratified viscoelastic media and its implication in tectonics and orogenesis. *Bull. geol. Soc. Am.* **72**, 1595–1620.

Biot, M. A. 1968. Edge buckling of a laminated medium. *Int. J. Solids Structures.* **4**, 125–137.

Biot, M. A., Odé, H. & Roever, W. L. 1961. Experimental verification of the theory of folding of stratified viscoelastic media. *Bull geol. Soc. Am.* **72**, 1621–1632.

Borradaile, G. J. 1972. Variably oriented co-planar primary folds. *Geol. Mag.* **109**, 89–98.

Bryant, B. & J. C. Reed, J. 1969. Significance of lineation and minor folds near major thrust faults in the southern Appalachians and the British and Norwegian Caledonides. *Geol. Mag.* **106**, 412–429.

Carreras, J., Estrada, A. & White, S. 1977. The effects of folding on the *c*-axis fabrics of a quartz mylonite. *Tectonophysics* **39**, 3–24.

Chapple, W. M. 1968. A mathematical theory of finite-amplitude rock-folding. *Bull. geol. Soc. Am.* **79**, 48–68.

Cloos, E. 1946. Lineation. A critical review and annotated bibliography. *Mem. geol. Soc. Am.* **18**, 122.

Cobbold, P. R. 1975. Fold propagation in single embedded layers. *Tectonophysics* **27**, 333–351.

Cobbold, P. R. & Quinquis, H. 1980. Development of sheath folds in shear regimes. *J. Struct. Geol.* **2**, 119–126.

Cobbold, P. R. & Watkinson, A. J. 1981. Bending anisotropy: a mechanical constraint on the orientation of fold axes in an anisotropic medium. *Tectonophysics* **72**, T1–T10.

Davis, G. A. & Lister, G. S. 1988. Detachment faulting in continental extension; perspectives from the southwestern U.S. Cordillera. *Spec. Pap. Geol. Soc. Am.* **128**, 133–159.

Donath, F. A. & Parker, R. B. 1964. Folds and folding. *Bull. geol. Soc. Am.* **75**, 45–62.

Escher, A. & Watterson, J. 1974. Stretching fabrics, folds and crustal shortening. *Tectonophysics* **22**, 223–231.

Fletcher, R. C. 1974. Wavelength selection in the folding of a single layer with power-law rheology. *Am. J. Sci.* **274**, 1029–1043.

Fletcher, R. C. 1991. Three-dimensional folding of an embedded viscous layer in pure shear. *J. Struct. Geol.* **13**, 87–96.

Fletcher, R. C. & Sherwin, J. 1978. Arc lengths of single layer folds: a discussion of the comparison between theory and observation. *Am. J. Sci.* **278**, 1085–1098.

Flinn, D. 1962. On folding during three-dimensional progressive deformation. *Q. J. geol. Soc. Lond.* **118**, 385–433.

Froitzheim, N. 1992. Formation of recumbent folds during synorogenic crustal extension (Austroalpine nappes, Switzerland). *Geology* **20**, 923–926.

Ghosh, S. K. 1970. A theoretical study of intersecting fold patterns. *Tectonophysics* **9**, 559–569.

Ghosh, S. K. 1974. Strain distribution in superposed buckling folds and the problem of reorientation of early lineations. *Tectonophysics* **21**, 249–272.

Gilotti, J. A. & Hull, J. M. 1993. Kinematic stratification in the hinterland of the central Scandinavian Caledonides. *J. Struct. Geol.* **15**, 629–646.

Grujic, D. 1992. Superposed folding: analogue models and comparison with natural examples from the Maggia nappe (Pennine Zone, Switzerland). Unpublished Ph.D. thesis, ETH Zürich, Switzerland.

Grujic, D. 1993. The influence of initial fold geometry on Type 1 and Type 2 interference patterns: an experimental approach. *J. Struct. Geol.* **15**, 293–307.

Hobbs, B. E. 1972. Deformation of non-Newtonian materials in simple shear. In: *Flow and Fracture of Rocks* (edited by Heard, H. C., Borg, I. Y., Carter, N. L. & Raleigh, C. B.). *Geophys. monograph* **16**, 243–258.

Huber-Alefi, A. 1982. Strain determinations in the conglomeratic gneiss of the Lebendun Nappe, Ticino, Switzerland. *Geologica Rom.* **21**, 235–277.

Hudleston, P. J. 1973. An analysis of 'single-layer' folds developed experimentally in viscous media. *Tectonophysics* **16**, 189–214.

Hudleston, P. J. 1977. Similar folds, recumbent folds and gravity tectonics in ice and rocks. *J. Geol.* **85**, 113–122.

Hudleston, P. J. 1986. Extracting information from folds in rocks. *J. Geol. Education.* **34**, 237–245.

Hudleston, P. J. & Lan, L. 1993. Information from fold shapes. *J. Struct. Geol.* **15**, 253–264.

Ildefonse, B. & Mancktelow, N. S. 1993. Deformation around rigid particles: the influence of slip at the particle/matrix interface. *Tectonophysics* **221**, 345–359.

James, A. I. & Watkinson, A. J. 1994. Initiation of folding and boudinage in wrench shear and transpression. *J. Struct. Geol.* **16**, 883–893.

Kirby, S. H. 1985. Rock mechanics observations pertinent to the rheology of the continental lithosphere and the localization of strain along shear zones. *Tectonophysics* **119**, 1–27.

Klaper, E. M. 1988. Quartz *c*-axis fabric development and large-scale post-nape folding (Wandfluhhorn Fold, Penninic nappes). *J. Struct. Geol.* **10**, 795–802.

Malavieille, J. 1987. Extensional shearing deformation and kilometer-scale '*a*'-type folds in a Cordilleran metamorphic core complex (Raft River Mountains, Northwestern Utah). *Tectonics* **6**, 423–448.

Mancktelow, N. S. 1988a. An automated machine for pure shear deformation of analogue materials in plane strain. *J. Struct. Geol.* **10**, 101–108.

Mancktelow, N. S. 1988b. The rheology of paraffin wax and its usefulness as an analogue for rocks. *Bull. geol. Instn. Univ. Upsala* **N.S. 14**, 181–193.

Mancktelow, N. S. 1990. The Simplon fault zone. *Beiträge zur Geologischen Karte der Schweiz.* **[N.F.] 163**.

Mancktelow, N. S. 1992. Neogene lateral extension during convergence in the Central Alps: evidence from interrelated faulting and backfolding around the Simplonpass (Switzerland). *Tectonophysics* **215**, 295–317.

Mancktelow, N. S. & Abbassi, M. R. 1992. Single layer buckle folding in non-linear materials—II. Comparison between theory and experiment. *J. Struct. Geol.* **14**, 105–120.

Mancktelow, N. S. & Pavlis, T. L. In press. Fold-fault relationships in low-angle detachment systems. *Tectonics.*

Mainz, R. & Wickham, J. 1978. Experimental analysis of folding in simple shear. *Tectonophysics* **44**, 79–90.

Mattauer, M. 1975. Sur le méchanisme de formation de la schistosité dans l'Himalaya. *Earth Planet. Sci. Lett.* **28**, 144–154.

Mazzoli, S. & Carnemolla, S. 1993. Effects of the superposition of compaction and tectonic strain during folding of a multilayer sequence—model and observations. *J. Struct. Geol.* **15**, 277–291.

Milnes, A. G. 1968. Strain analysis of the basement nappes in the Simplon region, northern Italy. *Rep. 23rd int. geol. Congr. Prague* **3**, 61–76.

Odonne, F. & Vialon, P. 1983. Analogue models of folds above a wrench fault. *Tectonophysics* **99**, 31–46.

Odonne, F. & Vialon, P. 1987. Hinge migration as a mechanism of superimposed folding. *J. Struct. Geol.* **9**, 835–844.

Ramberg, H. 1959. Evolution of ptygmatic folding. *Norsk. Geol. Tidsskr.* **39**, 99–152.

Ramberg, H. 1961. Contact strain and folding instability of a multilayered body under compression. *Geol. Rundsch.* **51**, 405–439.

Ramberg, H. 1964. Selective buckling of composite layers with contrasted rheological properties, a theory for simultaneous formation of several orders of folds. *Tectonophysics* **1**, 307–341.

Ramsay, J. G. 1967. *Folding and Fracturing of Rocks.* McGraw-Hill, New York.

Ramsay, J. G. & Huber, M. I. 1983. *The Techniques of Modern Structural Geology. Volume 1: Strain Analysis.* Academic Press, New York.

Ramsay, J. G. & Huber, M. I. 1987. *The Techniques of Modern Structural Geology. Volume 2: Folds and Fractures.* Academic Press, New York.

Ramsay, J. G. & Wood, D. S. 1973. The geometric effects of volume change during deformation processes. *Tectonophysics* **16**, 263–277.

Ridley, J. 1986. Parallel stretching lineations and fold axes oblique to a shear displacement direction—a model and observations. *J. Struct. Geol.* **8**, 647–653.

Ridley, J. & Casey, M. 1989. Numerical modeling of folding in rotational strain histories: strain regimes expected in thrust belts and shear zones. *Geology* **17**, 875–878.

Sanderson, D. J. 1973. The development of fold axes oblique to the regional trend. *Tectonophysics* **16**, 55–70.

Schäppi, H. 1985. Geologische Untersuchungen in der Valle Loana (Prov. Novara, Italien). Unpublished Diploma thesis, ETH Zürich, Switzerland.

Schmid, S. M., Zingg, A. & Handy, M. 1987. The kinematics of movement along the Insubric Line and the emplacement of the Ivrea Zone. *Tectonophysics* **135**, 47–66.

Sherwin, J. & Chapple, W. H. 1968. Wavelengths of single layer folds: a comparison between theory and observation. *Am. J. Sci.* **266**, 167–179.

Simpson, C. 1982. The structure of the northern lobe of the Maggia Nappe, Ticino, Switzerland. *Eclogae geol. Helv.* **75**, 495–516.

Skjernaa, L. 1980. Rotation and deformation of randomly oriented planar and linear structures in progressive simple shear. *J. Struct. Geol.* **2**, 101–109.

Smith, R. B. 1975. Unified theory of the onset of folding, boudinage, and mullion structure. *Bull. geol. Soc. Am.* **86**, 1601–1609.

Spencer, J. E. 1982. Origin of folds of Tertiary low-angle fault surfaces, southeastern California and western Arizona. In: *Mesozoic–Cenozoic Tectonic Evolution of the Colorado River Region California, Arizona and Nevada (Anderson-Hamilton volume)* (edited by Frost, E. G. & Martin, D. L.). Cordilleran Publishers, San Diego, 123–134.

Stünitz, H. 1991. Folding and shear deformation in quartzites, inferred from crystallographic preferred orientation and shape fabrics. *J. Struct. Geol.* **13**, 71–86.

Talbot, C. J. 1970. The minimum strain ellipsoid using deformed quartz veins. *Tectonophysics* **7**, 47–76.

Treagus, S. H. 1972. Processes in fold development. Ph.D. thesis (unpublished), University of Manchester, England.

Treagus, S. H. 1973. Buckling stability of a viscous single-layer system, oblique to the principal compression. *Tectonophysics* **19**, 271–289.

Treagus, S. H. & Sokoutis, D. 1992. Laboratory modelling of strain variation across rheological boundaries. *J. Struct. Geol.* **14**, 405–424.

Treagus, J. E. & Treagus, S. H. 1981. Folds and the strain ellipsoid: a general model. *J. Struct. Geol.* **3**, 1–17.

Watkinson, A. J. 1975. Multilayer folds initiated in bulk plane strain with the axis of no change perpendicular to the layering. *Tectonophysics* **28**, T7–T11.

Watkinson, A. J. & Cobbold, P. R. 1981. Axial direction of folds in rocks with linear/planar fabrics. *J. Struct. Geol.* **3**, 211–217.

Weijermars, R. 1986. Flow behaviour and physical chemistry of bouncing putties and related polymers in view of tectonic laboratory applications. *Tectonophysics* **124**, 325–358.

Wilcox, R. E., Harding, T. P. & Seely, D. R. 1973. Basic wrench tectonics. *Bull. Am. Ass. Petrol. Geol.* **57**, 74–96.

Williams, G. D. 1978. Rotation of contemporary folds into the X direction during overthrust processes in Lakesfjord, Finnmark. *Tectonophysics* **48**, 29–40.

Yin, A. 1991. Mechanisms for the formation of domal and basinal detachment faults: a three-dimensional analysis. *J. geophys. Res.* **96**, 14577–14594.